Predicting Bird Diversity with Lidar-derived Vegetation Structure in an African Savanna

Peter B. Boucher[1] and Andrew B. Davies[1,*]

[1] *Department of Organismic and Evolutionary Biology, Harvard University, 22 Divinity Avenue*

Cambridge, MA, USA 02138

**corresponding author*

pboucher@g.harvard.edu; andrew_davies@g.harvard.edu

Running title: Predicting diversity from vegetation structure

Abstract

Vegetation structural complexity and the diversity of animal communities are closely linked in vegetated ecosystems. These structure-diversity relationships have the potential to be used to predict biodiversity at large spatial scales using remote sensing data. However, structure-diversity relationships may not be generalizable across different ecosystems or even across ecotypes within a single ecosystem. To understand how structure-diversity relationships vary within the tree-grass mosaic of a savanna environment, we evaluated how bird diversity relates to vegetation structure at multiple scales and across environmental gradients in an East African savanna- the Selenkay Conservancy in southern Kenya. We obtained detailed characterizations of vegetation structure using Light Detection and Ranging (lidar) from Unoccupied Aerial Vehicle (UAV) surveys, and related vegetation structure metrics to bird diversity metrics (Shannon diversity and species richness) collected at 50 sites spread inside and outside of the Selenkay Conservancy. We compared structure-diversity relationships across environmental gradients, including soil type (red and black soils) and protected status (inside and outside the conservancy). We also compared structure-diversity models at multiple scales, testing how relationships changed with scale. We found significant structure-diversity relationships with improved performed at larger spatial scales (≥ 50 m radius or 0.79 ha circular plots). Models of Shannon diversity performed better than those of species richness. While most structure-diversity relationships only applied to specific soil types, certain models showed the potential to be generalized across soil types, explaining ~55-59% of the variance. We found that strong relationships exist between vegetation structure and bird diversity in savannas. While most structure-diversity relationships were only applicable to specific soil types, several vegetation metrics were able to track bird diversity across the entire landscape, performing well in both red

and black soil sites. These results demonstrate the potential to use airborne remote sensing to monitor biodiversity across savanna environments.

Keywords

unoccupied aerial vehicles, heterogeneity, complexity, biodiversity, Amboseli, nature-based solutions

Introduction

Biodiversity monitoring has largely relied on field observations taken by highly trained survey guides, but new technologies, including camera traps (Steenweg et al., 2017), audio recordings (Aide et al., 2013; Pekin et al., 2012; Rappaport et al., 2020), and remote sensing (Davies & Asner, 2014; Moudrý et al., 2022; Simonson et al., 2014) have the potential to revolutionize methods for measuring species counts and biodiversity metrics. These exciting new developments could enable researchers, companies, and governments to track both loss and uplift of biodiversity at large scales, offering potential new pathways for valuing biodiversity and the ecosystem services it provides (Berzaghi et al., 2019; Schmitz et al., 2023). With governments beginning to recognize biodiversity as a global resource (Kunming-Montreal Global Biodiversity Framework, 2022), these monitoring technologies have great potential for use in conservation and nature-based solutions (NBS) projects worldwide.

Remote sensing technologies have been highlighted as particularly adept tools for measuring proxies of biodiversity, offering the potential to map biodiversity at landscape scales. Studies have demonstrated the strong correlation between remotely sensed measures of vegetation complexity and animal (Bae et al., 2019; Bonn et al., 2004; Davies & Asner, 2014; Goetz et al., 2007), plant (Coverdale & Davies, 2023; Guo et al., 2017; Marselis et al., 2019), and acoustic

diversity (Pekin et al., 2012; Rappaport et al., 2020). The theoretical basis for these studies largely relies on the habitat-heterogeneity hypothesis (MacArthur & MacArthur, 1961), which predicts that ecosystems with more complex structures have more ecological niches and therefore host a higher diversity of animal and plant species. Research on bird communities has built particularly strong support for this theory, showing that areas with higher vegetation productivity and structural complexity (Bonn et al., 2004; Carrasco et al., 2019; Goetz et al., 2007; MacArthur & MacArthur, 1961) have more diverse avian communities.

Airborne light detection and ranging (lidar) surveys provide an efficient means to monitor vegetation complexity as a proxy for biodiversity across large extents (Davies & Asner, 2014; Moudrý et al., 2022; Simonson et al., 2014). Lidar is an active remote sensing technology that emits pulses of light to sample environments, producing 3-D reconstructions of vegetation structure and topography (Gatziolis & Andersen, 2008). Lidar sensors are particularly well-suited for biodiversity monitoring due to their ability to measure aspects of the vertical profile of multilayered vegetation that are influential for biodiversity, including structural indices derived from ratios of vegetation height, and measures of the variation in vegetation complexity across an area (Boucher et al., 2023; Davies et al., 2019, 2020; Davies & Asner, 2014; LaRue et al., 2020; Moudrý et al., 2022).

While there are clear links between lidar data and biodiversity measures, practical challenges to monitoring biodiversity with vegetation structure at large scales remain. Structure-diversity relationships measured with remote sensing may need to be localized and calibrated toward specific animal or plant communities, as well as to local environmental gradients. Ecological communities respond to environmental gradients at a variety of spatial and temporal scales (Jackson & Fahrig, 2015; Levin, 1992; McGarigal & Marks, 1995). Therefore, a remote-sensing-

based biodiversity survey needs to be detailed enough to capture vegetation structure at the spatial scales and temporal resolutions that are most pertinent to the ecological communities of interest. Similarly, structure-diversity relationships may not be universally applicable across environmental gradients and ecoregions. Most remote sensing studies of biodiversity relationships have been conducted in temperate and tropical forest environments (Davies & Asner, 2014). However, the same models of structure-diversity trained in forested environments might not apply to other environments and climates, such as grasslands and savannas. Yet biodiversity monitoring technologies and valuation schemes could be of particular benefit in African savannas and grasslands, where, historically, ecosystem services have been greatly undervalued (Bond et al., 2019; Veldman et al., 2015).

Here, we explore how remote sensing biodiversity monitoring methods might operate in a non-forested, mosaicked ecosystem by evaluating structure-diversity relationships in an East African savanna: the Selenkay Conservancy in southern Kenya. As a small, protected area set aside for ecotourism within a larger mixed-use landscape, the Selenkay Conservancy provides a gradient of human activity and wildlife density within a small area (~5,000 hectares) that can be easily covered using airborne remote sensing surveys. We surveyed vegetation structure with unoccupied aerial vehicle (UAV) lidar surveys and sampled bird diversity with field observations, stratifying samples along gradients of protected status (inside and outside the conservancy) and soil type (red and black soils). We evaluated models of structure-diversity across these environmental gradients, modelling bird diversity (species richness and the Shannon-Wiener Index) with vegetation structure metrics derived from lidar data at a variety of scales. By searching for generalized models of biodiversity relationships in a savanna

environment, we explore the feasibility of utilizing airborne remote sensing for monitoring biodiversity across environmental gradients in non-forested ecosystems.

Materials and Methods

Study Site

The core wildlife area of the Selenkay Conservancy is a 5,260 ha protected area in southern Kenya, ~30 km north of Amboseli National Park (Fig. 1). The conservancy sits within a larger (~81,000 ha) collection of private lands primarily owned by members of indigenous Maasai communities who practice subsistence agriculture (outside the conservancy) and rotational livestock grazing (inside and outside the conservancy). The unfenced conservancy has been leased and managed by an ecotourism company, Gamewatchers Safari Ltd, since 1997. Other than a small, tented camp, dirt roads, some temporary livestock enclosures (bomas) and several man-made water sources, there is little development within the conservancy. In contrast, the outside area is generally considered to be degraded due to over-grazing from livestock and an abundance of invasive plant species, such as the common morning glory, *Ipomoea purpurea*.

While rainfall is highly variable and droughts are common in the region (Tuqa et al., 2014; Altman et al., 2002), there are generally 2 wet seasons a year, approximately from March-May and October-December, and 2 dry seasons, from January-February and June-September. The terrain around the conservancy is relatively flat, with a range of ~120 m in elevation across the sampled area. The geology consists of 2 dominant soil types: black cotton soil, which retains moisture well, and red soils, which do not. These different geologies support different vegetation communities (Goheen et al., 2018).

UAV Lidar Data Collection

UAV lidar surveys were conducted over the course of 5 days during the beginning of the short dry season (5-9 Jan 2022). UAV survey extents were designed to capture both the protected area inside the conservancy and areas outside of the conservancy (Fig. 1). The UAV sampling design employed 5 circular surveys of ~2 km radius (covering ~1,800 ha area each) along with an additional survey of a smaller 723 ha area. Survey sites were designed to capture approximately equal areas of black and red soil.

UAV surveys were conducted with a Freefly Alta-X multirotor carrying the Harvard Animal Landscape Observatory (HALO), a sensor package designed for high resolution characterization of landscape structure (Boucher et al., 2023). Developed by Phoenix Lidar Systems in Los Angeles, California, USA, HALO integrates a Riegl VUX-1LR lidar, a FLIR Tau-2 thermal imager, and a Sony A6000 camera with an advanced positioning system. Survey flights were planned and deployed autonomously using the QGroundControl software application, with a certified pilot manually conducting take-offs and landings. Flight and lidar sensor settings were parameterized with Riparameter 2.2 and Phoenix Lidar System's Spatial Explorer 6.0. The UAV was flown at 8 m/s and at an altitude of 120 m above ground level to maximize area coverage while adhering to the Kenya Civil Aviation Authority (KCAA) regulations. The pulse rate of the lidar scanner was set to 820 kHz and the line speed was 78.1 lines per second.

Raw point clouds were denoised, and points were classified into ground and vegetation in Spatial Explorer 6.0 and the Terrasolid software suite. After processing, the resulting point density of the lidar data ranged from 201-234 points per m^2 (Table S1), and the relative accuracy of the processed point clouds was ~3 cm or better.

Bird Diversity Surveys

Bird surveys were conducted twice a day over the course of 20 days at the beginning of the long dry season, from June 18-27 and July 1-10, at dawn (6:00 – 8:00) and dusk (16:00 – 19:00). Following Asefa et al. (2017), survey sites were laid out along 10 transects of 1-1.5 km each, with 5 sites on each transect. Transect locations were placed randomly within the boundaries of each lidar survey and stratified equally across soil types. Six transects were placed inside the conservancy, and 4 outside. Site locations were spaced ~300 m apart along a North-South axis, but several sites were adjusted to fit within the circular area of the lidar surveys and to facilitate access (Fig. 1). Each site was surveyed twice at dawn and twice at dusk. Surveys lasted ten minutes per site, with an additional two minutes of quiet time before data collection began. Observations were recorded at the center position of each site following Asefa et al. (2017), and bird species were identified both by sight and sound by trained ecotourism guides who were highly knowledgeable of the local bird species. Species observations and abundances were recorded in the field using a custom-built surveying application. Raw observations were aggregated by species, pooling the data collected across all time periods and observers.

Bird observational data were processed into diversity statistics, and the species richness, total abundance, Shannon-Wiener index, and Pielous's evenness (Oksanen, 2022) were calculated and compared across all 50 sites. To reduce the impact of extremely rare sightings on the diversity metrics, we removed records of bird species that were observed only once across all sites and throughout the entire 20-day survey. A nested ANOVA was used to test for significant differences between sites, grouped by soil type and protected status. In addition, a non-metric multidimensional scaling (NMDS) ordination with Bray-Curtis dissimilarity distances (Bray &

Curtis, 1957) was performed to examine variation in bird communities by soil type and protected status. NMDS and diversity statistics were computed using the *vegan* package in R (Oksanen, 2022).

Lidar Vegetation Metrics

To examine relationships between lidar vegetation metrics at multiple scales, we computed vegetation metrics within circular plots centered on the 50 bird diversity sites (similar to the methods in Sangermano, 2022). We derived sets of lidar metrics at 6 scales, using circular plots with 10 m, 20 m, 30 m, 50 m, 80 m, and 130 m radius buffers (Fig. 1c). Structural metrics were calculated from the processed point clouds following the workflow in *Lidar-Notebooks* (https://github.com/pbb2291/Lidar-Notebooks), a pipeline for deriving vegetation metrics from point clouds and polygons in python and jupyter notebooks.

After reviewing previous studies of structure-diversity relationships (Bae et al., 2019; Goetz et al., 2007; Rappaport et al., 2020), a myriad of vegetation structural complexity metrics were identified for further analysis (Table S2). These metrics were selected to capture a variety of aspects of vegetation heterogeneity, including vertical and horizontal variation in vegetation height, density, layering, density, and plant composition (horizontal cover of pixels classified as trees, grasses, and shrubs). Metrics were summarized for each site in 2 ways: 1) as plot-based metrics calculated from the vertical distribution of all lidar points within a plot (Fig. 2a and 2c) and 2) as pixel-based statistics that describe the mean, standard deviation, and coefficient of variation of metrics rasterized at a horizontal spatial resolution of 0.5 m (Fig. 2b). Plot-based metrics describe the aggregated structure of all vegetation within a plot, whereas pixel-based metrics describe the spatial variation and average metrics across a plot. The difference between

plot-based and pixel-based metrics is akin to the difference between large-footprint waveform lidar, which measures the aggregate metrics of a whole stand of trees within a single beam, and small-footprint lidar, which captures the structural details of individual trees, branches, and leaves (Boucher et al., 2020). With the full set of plot and pixel-based metrics, a total of 114 variables were derived to describe the vegetation structure of each plot (Table S2).

Analysis of Structure-Diversity Relationships

To examine relationships between bird diversity and vegetation metrics at increasingly larger scales, we calculated the pairwise Spearman rank correlation between lidar vegetation metrics and bird species richness, and between the vegetation metrics and the Shannon diversity index, comparing the magnitude and direction of correlations across the series of increasing scales. We expected that structure-diversity relationships would also be influenced by soil type, and we therefore conducted separate correlation analyses for black and red soils (n = 25 sites per soil type) and examined the top variables for both diversity metrics within each soil type.

We then fit Generalized Additive Models (GAMs) of Shannon diversity and log-transformed species richness at each scale, using the top 3 most correlated variables from each soil type and each scale as the independent variables in the models. GAMs have been successfully employed in previous studies to model non-linear relationships between structure and diversity (Bae et al., 2019) and combine the robustness of Generalized Linear Models (GLMs) with the flexibility of black-box machine learning models (Wood, 2017). GAMs use a series of smoothing splines to model relationships between variables, employing a penalty to reduce the wiggliness of the splines and thereby prevent overfitting. GAMs can also penalize unimportant features in a similar manner to ridge regression, dampening the effect of

insignificant variables. We used the *mgcv* package in R (Wood, 2017) to model species diversity and richness, fitting a GAM model for each of the 6 scales. To account for spatial autocorrelation, each model included a term to describe the interaction between the easting and northing locations of each site (*s(X,Y)*).

Results

Bird Community Analysis

After filtering bird species records for rare observations (by dropping species with only 1 occurrence in the entire dataset), a total of 8,237 individual birds from 129 species were recorded across all sites and time periods. In aggregate, similar numbers of birds were observed within each soil type, with 4,217 observations from 114 species in black soils and 4,020 counts from 112 species in red soils (Table 1), with nested ANOVA results showing that there was not a significant difference in the mean abundance ($p = 0.466$) nor richness ($p = 0.457$) between soil types. However, the evenness of communities on black soil sites was significantly lower than red soil sites ($p = 0.041$), most likely because of the high evenness in red soil sites outside the conservancy (Fig. 3). Potentially, black soils also had lower Shannon diversity than red soil sites ($p = 0.07$).

The average abundance, richness, and Shannon diversity of sites were generally higher inside the conservancy than outside (Table 1; Fig. 3). There was a significant effect of protected status within soil types for abundance ($p = 0.02$), richness ($p = 0.01$), and potentially also for evenness ($p = 0.06$), but not for Shannon diversity ($p = 0.22$).

NMDS ordination analyses indicated that bird assemblage compositions were clustered and grouped by both soil type and protected status (Fig. 4). A visualization of the first 2 NMDS

axes for all sites showed that bird communities tended to be more similar among sites with similar soil types (Fig. 4a). In addition, within each soil type, communities tended to be more similar among sites that shared the same protected status (Fig. 4b and 4c). The NMDS ordinations used 3 dimensions, and the resulting stress values were 0.17 for an ordination with all sites, 0.14 with black soil sites only, and 0.13 with red soil sites.

Correlation of Structure and Diversity by Scale

Correlations between UAV-lidar vegetation metrics and both species richness and Shannon diversity index were generally higher in black soils than red soils (Tables 2 and 3, Fig. 5). For Shannon diversity, the strongest correlation for black soils occurred at a 50 m scale (ρ=0.83, $p<0.001$) before plateauing, while the strongest correlation in red soils was at a 130 m scale (ρ=0.52, p=0.002; Table 2, Fig. 5). The strength of correlations with species richness were more similar across soil types, but in opposing directions. The strongest correlation in black soils occurred at a 50 m scale with a positive trend (ρ=0.69, $p<0.001$), while in red soils, the strongest correlation occurred at the 80 m and 130 m scales with a negative trend (ρ=-0.67, p=0.001*;* Table 3, Fig. 5).

The sets of variables that demonstrated the strongest correlations with Shannon diversity and species richness also varied by soil type. For Shannon diversity, vegetation metrics derived from the vertical profile of lidar returns, such as statistics of the height of points (*meanH_plot*), the distribution of peaks in the vertical profile (*mean_gapsize*, *sd_gapsize*, and *mean_stdpeakh*), and the canopy density (*CD1p5m_plot*), were highly correlated with the Shannon index (Table 2). The top variables for black soils had a mix of plot-based and pixel-based metrics, while the top variables for red soils were all plot-based metrics (Table 2). For species richness, the set of

highly correlated variables was different between black and red soils (Table 3). The top variables in black soils were measures of the average of (*meanH_plot*) and variation in vegetation complexity (*sdH_plot*, *cv_nlayers*, and *sd_nlayers*), particularly for taller, woody vegetation. In contrast, red soils showed a strong correlation with heterogeneity in the grass layer (*horzcover_grass*, *sd_sdH_vegtype_grass,* and *sd_cvH_vegtype_grass*).

Models of Structure and Diversity by Scale

In general, models of Shannon diversity and log-transformed species richness tended to improve with increasing scale. As the scale expanded from 10 m to 130 m, the R^2 and explained deviance values of models increased, and the AIC and RMSE values decreased (Tables 4 and 5). Among the Shannon diversity (Table 4 and S3) and species richness (Table 5 and S4) models, the 50 m and 130 m models had the lowest errors and the highest correlations; the same scales that exhibited the strongest correlations in the pairwise correlation analysis (Tables 2 and 3). Both pixel-based and plot-based metrics of vegetation structure were found to be significant predictors of Shannon diversity and species richness (Tables 4 and 5).

For Shannon diversity (Table 4), significant pixel-based metrics included: the standard deviation and coefficient of variation in canopy density at 25 cm above ground (*sd_CD_AboveG, cv_CD_AboveG*), and the mean and variation of various height statistics and indices derived from the vertical profile of point density (*mean_gapsize, mean_stdpeakh, sd_gapsize,* and *sd_herbh*). Important plot-based metrics included: the canopy density value of the entire plot at 0.5 m and 1.5 m above ground (*Cover0p5m_plot*, *Cover1p5m_plot*) and vegetation height indices derived from the peaks in the vertical profile of the point density (*VDRpeak_plot, cv_FHD,* and *cvpeakh_plot*). The spatial autocorrelation term was not found to be a significant

variable in any of the Shannon diversity models ($p > 0.05$), but it approached significance in the 80 m model ($p = 0.06$).

Models of species richness had lower R^2 values and higher error statistics compared to models of Shannon diversity, even at larger scales. Richness models reached a maximum R^2 of 0.39 (Table 5), while Shannon models reached a maximum R^2 of 0.59 (Table 4). Richness models contained some of the same independent variables as the models of Shannon diversity (Table 5), including the variation in gap size (*sd_gapsize*), a canopy height index (*VDRpeak_plot*), and the variation in the heights of canopy layers (*cvpeakh_plot*). However, richness models also incorporated other vegetation structure metrics, including the proportion of area covered by grasses (*horzcover_grass*), the variation in canopy density (*cv_CD_AboveG*), and the variation in the number and height of canopy layers (*sd_nlayers)*. The spatial autocorrelation term also had more of an effect in richness models, particularly at the 20 m and 30 m scales (Table 5).

A simplified version of the best model of Shannon diversity at 130 m (Table 4) demonstrates how vegetation heterogeneity, measured as the pixel-wise standard deviation in gap size (*sd_gapsize*), varies with Shannon diversity (Fig. 6). The standard deviation in gap size, a metric describing the maximum vertical distance between canopy layers (Fig. 2c and Fig. S1), increases with Shannon diversity up to 1 m, where the function reaches an inflection point and begins to decrease (Fig. 6). This concave downward trend shows that variation in gap size increases with bird diversity up to a point, after which increasing heterogeneity is indicative of lower, rather than higher Shannon diversity. The increasing trend between gap size variation and Shannon diversity appears to be driven largely by the influence of black soil sites, while the decreasing trend seems to be due to the influence of red soil sites (Fig. 6).

Using the model of gap size at 130 m scale, Shannon diversity was then predicted across a larger 3 km x 2 km area within the northwest region of the conservancy at 260 m spatial resolution (Fig. 7). This map demonstrates how structure-diversity models could be used to predict biodiversity at larger scales, revealing hotspots of Shannon diversity across a large area (Fig. 7).

Discussion

Our results reveal that bird diversity metrics are strongly (R^2 = ~0.6) correlated with vegetation structure, particularly at larger scales (≥ 50 m radius or ≥ 0.79 ha plots). The structure-diversity relationships we observed at Selenkay involved similar structural metrics to those reported in previous studies in temperate and tropical forests (Bae et al., 2019; Goetz et al., 2007; Moudrý et al., 2022; Pekin et al., 2012; Rappaport et al., 2020), which suggests potential for predicting spatial variation in biodiversity with lidar in multiple vegetated ecosystems around the world. However, our results also highlight that vegetation structure-diversity relationships are not identical across ecosystems, but rather vary with ecotypes.

At Selenkay, soil type played a particularly strong role in determining structure-diversity relationships. Each soil type had unique avian communities (Fig. 4a) and different spatial arrangements of vegetation, which led to variable relationships between vegetation structure and diversity in each soil type (Fig. 5). The scales and sets of variables for modelling bird diversity in black soil sites were also different from those in red soils, and correlations between structure and diversity metrics were generally higher in black soils (Tables 2 and 3). Furthermore, when plotting metric correlations with Shannon diversity by scale (Fig. 5), correlations in black soils stabilized and reached an asymptote at the 50 m scale (0.8 ha plots), whereas they did not

stabilize in red soils, even at the 130 m scale (5.3 ha plots). The differences in structure-diversity relationships in black and red soils are likely indicative of differences in the spatial arrangement of vegetation between the soil types, with vegetation structure on black soils generally being more homogenous.

The different structure-diversity relationships observed within each soil type demonstrate that certain models may not perform well across ecotypes, implying that biodiversity monitoring efforts that aim to scale up structure-diversity models to regional scales need to develop and implement ecotype-specific models. However, our results also reveal that certain vegetation metrics have greater potential for predicting biodiversity across soil types, particularly at larger scales. The 50 m (0.8 ha) and 130 m (5.3 ha) models of Shannon diversity performed relatively well across both soil types ($R^2 \geq 0.56$, RMSE = ~0.1; Table 4), with the 130 m model of the variation in gap size being particularly promising (Figs. 6 and 7).

Gap size describes the distance between vertical layers within multilayered vegetation (Fig. 2c), and the standard deviation in gap size (*sd_gapsize*) describes the magnitude of its variation across the landscape, which is related to the height, complexity, and horizontal cover of multi-layered vegetation in an area. Variation in gap size, therefore, can be understood as a generalized measure of vegetation heterogeneity. At Selenkay, the variation in gap size increases with Shannon diversity, largely due to the influence of the black soil sites, until the trend reaches an inflection point where red soil sites cause a decreasing trend between gap size variation and diversity (Fig. 6). These differing trends in black and red soils have interesting implications for the habitat-heterogeneity (H-H) hypothesis, which posits that biodiversity increases with increased heterogeneity due to a larger number of ecological niches (MacArthur & MacArthur, 1961). Vegetation heterogeneity increased with diversity in black soil sites, confirming the H-H

hypothesis, while heterogeneity decreased with diversity in red soil sites, opposing it. Black soil sites tend to be much more homogenous in their vegetation structure relative to res soil sites (Figure 5), and bird assemblages within black soils therefore likely benefit from increased structural heterogeneity. In contrast, bird assemblages in the more heterogenous red soil environment could find increased heterogeneity to lead extreme heterogeneity that is detrimental to diversity because it favors certain species over others. Diversity-heterogeneity relationships may therefore be hump-shaped in much the same way as diversity-productivity relationships are (Mittleback et al., 2001). Overall, however, we found that the gap size metric is a promising predictor of diversity, and more field data from red soil sites with a wider range of diversity values could help confirm its applicability across soil types.

More broadly, vegetation structure metrics that performed well for modeling diversity at Selenkay were those derived from the vertical profile of the distribution of lidar points (Fig. 2c). Metrics related to the variation of peaks in the vertical profile, including the number of canopy layers, the peak height values, and the gap size, were often selected as the top variables in the models. These important variables described the spatial variation of these vertical profile metrics across an area, calculated as the pixel-wise standard deviation or coefficient of variation of the metrics at a 0.5 m spatial resolution.

Promisingly, the vegetation structure metrics that related to bird diversity at Selenkay were similar to variables selected by previous studies of animal diversity in forest ecosystems in other regions of the world (Table S2). For example, canopy density was identified as an important metric for habitat suitability and animal diversity in European forests (Bae et al., 2019; Moudrý et al., 2022). In addition, we found certain ratio measures of canopy height used in previous studies to be important, such as the vertical distribution ratio (VDR) used by Goetz et

al. (2007) in a study of bird diversity in the eastern United States. Similarly, important measures of vertical complexity, such as the vertical gap size, were similar to a canopy gap metric identified in a study of acoustic diversity in a tropical Costa Rican rainforest (Pekin et al., 2012). The similar sets of metrics used among these studies bolsters support for the habitat-heterogeneity hypothesis (MacArthur & MacArthur, 1961) and demonstrates the potential to utilize airborne lidar to monitor biodiversity across a variety of vegetated ecosystems.

Implications for Biodiversity Monitoring

While comparing models of species richness and Shannon diversity, we found that models of richness (Table 5) did not perform as well as those for Shannon diversity (Table 4). The maximum R^2 achieved in models of richness, 0.39 at the 130 m scale, was considerably lower than that achieved for Shannon diversity, 0.59 at 130 m scale, even though both models used the same independent variable (*sd_gapsize*). The success of Shannon diversity models shows the importance of relying on numerous aspects of community structure in a biodiversity survey, focusing on more than just the number of species within a site (i.e., species richness). The Shannon index takes multiple aspects of community structure into account to produce a normalized diversity score, summarizing species counts, evenness, and relative abundances within an area. Accounting for these aspects greatly improved the Shannon structure-diversity models relative to the richness models. It is likely that species abundance and evenness also covaried with vegetation structure metrics, causing the improvement observed in the Shannon model scores. Therefore, we suggest that future biodiversity monitoring efforts use Shannon diversity or similar indices that combine species abundance, richness, and evenness to map diversity at landscape-scales.

However, our results also demonstrate that the Shannon index can be misleading when comparing biodiversity among sites. While evaluating bird community statistics within the Selenkay ecosystem, we found that both species abundance and richness were significantly lower outside the conservancy compared to inside (Fig. 3), suggesting that bird communities outside of Selenkay were less diverse than those inside. In contrast, when comparing Shannon diversity values, sites inside the conservancy were not significantly different from those outside, a result which is most likely due to differences in the evenness of bird communities among red soil sites inside and outside the conservancy (Fig. 3). If a monitoring study had relied on Shannon diversity alone to measure the status of bird communities at Selenkay, it might conclude that there is no significant difference in community structure inside and outside of the conservancy. Thus, relying on Shannon diversity alone would lead to a false-negative conclusion about the diversity among sites in this region. This result is highly informative for future biodiversity monitoring efforts, as it highlights the importance of relying on more than one diversity metric or analysis of community structure to make inferences about the diversity of an ecosystem relative to another.

By evaluating relationships between bird diversity and vegetation metrics in an African savanna, our study demonstrates the feasibility of predicting spatial patterns of biodiversity across non-forested landscapes with high-resolution remote sensing data. In the context of the many previous studies that have modelled structure-diversity relationships in tropical and temperature forests, our results show the potential to expand biodiversity monitoring efforts across a variety of biomes and ecoregions. The ability to map biodiversity across landscapes opens myriad new avenues of scientific research on the spatial and temporal drivers of biodiversity. In addition, these methods show great potential for monitoring biodiversity in the

context of addressing the global biodiversity crisis, providing a means to measure biodiversity uplift and loss over time and to monitor areas so that they can be managed with specific biodiversity targets in mind.

References

Aide, T. M., Corrada-Bravo, C., Campos-Cerqueira, M., Milan, C., Vega, G., & Alvarez, R. (2013). Real-time bioacoustics monitoring and automated species identification. *PeerJ*, *2013*(1), e103. https://doi.org/10.7717/PEERJ.103/FIG-4

Asefa, A., Davies, A. B., McKechnie, A. E., Kinahan, A. A., & van Rensburg, B. J. (2017). Effects of anthropogenic disturbance on bird diversity in Ethiopian montane forests. *The Condor*, *119*(3), 416–430. https://doi.org/10.1650/CONDOR-16-81.1

Bae, S., Levick, S. R., Heidrich, L., Magdon, P., Leutner, B. F., Wöllauer, S., Serebryanyk, A., Nauss, T., Krzystek, P., Gossner, M. M., Schall, P., Heibl, C., Bässler, C., Doerfler, I., Schulze, E. D., Krah, F. S., Culmsee, H., Jung, K., Heurich, M., … Müller, J. (2019). Radar vision in the mapping of forest biodiversity from space. *Nature Communications*, *10*(1), 10. https://doi.org/10.1038/s41467-019-12737-x

Berzaghi, F., Longo, M., Ciais, P., Blake, S., Bretagnolle, F., Vieira, S., Scaranello, M., Scarascia-Mugnozza, G., & Doughty, C. E. (2019). Carbon stocks in central African forests enhanced by elephant disturbance. *Nature Geoscience*, *12*(9), 725–729. https://doi.org/10.1038/s41561-019-0395-6

Bond, W. J., Stevens, N., Midgley, G. F., & Lehmann, C. E. R. (2019). The Trouble with Trees: Afforestation Plans for Africa. *Trends in Ecology & Evolution*, *34*(11), 963–965. https://doi.org/10.1016/J.TREE.2019.08.003

Bonn, A., Storch, D., & Gaston, K. J. (2004). Structure of the species-energy relationship.

Proceedings of the Royal Society B: Biological Sciences, *271*(1549), 1685–1691. https://doi.org/10.1098/RSPB.2004.2745

Boucher, P. B., Hockridge, E. G., Singh, J., & Davies, A. B. (2023). Flying high: Sampling savanna vegetation with UAV-lidar. *Methods in Ecology and Evolution*, *00*, 1–19. https://doi.org/10.1111/2041-210X.14081

Boucher, P., Hancock, S., Orwig, D., Duncanson, L., Armston, J., Tang, H., Krause, K., Cook, B., Paynter, I., Li, Z., Elmes, A., & Schaaf, C. (2020). Detecting Change in Forest Structure with Simulated GEDI Lidar Waveforms: A Case Study of the Hemlock Woolly Adelgid (HWA; Adelges tsugae) Infestation. *Remote Sensing*, *12*(8), 1304. https://doi.org/10.3390/rs12081304

Bray, J. R., & Curtis, J. T. (1957). An Ordination of the Upland Forest Communities of Southern Wisconsin. *Ecological Monographs*, *27*(4), 325–349.

Carrasco, L., Giam, X., Papęs, M., & Sheldon, K. S. (2019). Metrics of lidar-derived 3D vegetation structure reveal contrasting effects of horizontal and vertical forest heterogeneity on bird species richness. *Remote Sensing*, *11*(7), 1–19. https://doi.org/10.3390/rs11070743

CloudCompare (version 2.11). (2018). GPL Software. http://www.cloudcompare.org/

Coverdale, T. C., & Davies, A. B. (2023). Unravelling the relationship between plant diversity and vegetation structural complexity: A review and theoretical framework. *Journal of Ecology*. https://doi.org/10.1111/1365-2745.14068

Davies, A. B., & Asner, G. P. (2014). Advances in animal ecology from 3D-LiDAR ecosystem mapping. *Trends in Ecology & Evolution*, *29*(12), 681–691. https://doi.org/10.1016/j.tree.2014.10.005

Davies, A. B., Brodrick, P. G., Parr, C. L., & Asner, G. P. (2020). Resistance of mound-building

termites to anthropogenic land-use change. *Environmental Research Letters*, *15*(9), 094038. https://doi.org/10.1088/1748-9326/ABA0FF

Davies, A. B., Oram, F., Ancrenaz, M., & Asner, G. P. (2019). Combining behavioural and LiDAR data to reveal relationships between canopy structure and orangutan nest site selection in disturbed forests. *Biological Conservation*, *232*, 97–107. https://doi.org/10.1016/j.biocon.2019.01.032

Gatziolis, D., & Andersen, H.-E. (2008). *A Guide to LIDAR Data Acquisition and Processing for the Forests of the Pacific Northwest. Gen. Tech. Rep. PNW-GTR-768.* https://www.fs.fed.us/pnw/pubs/pnw_gtr768.pdf

Goetz, S., Steinberg, D., Dubayah, R., & Blair, B. (2007). Laser remote sensing of canopy habitat heterogeneity as a predictor of bird species richness in an eastern temperate forest, USA. *Remote Sensing of Environment*, *108*(3), 254–263. https://doi.org/10.1016/j.rse.2006.11.016

Goheen, J. R., Augustine, D. J., Veblen, K. E., Kimuyu, D. M., Palmer, T. M., Porensky, L. M., Pringle, R. M., Ratnam, J., Riginos, C., Sankaran, M., Ford, A. T., Hassan, A. A., Jakopak, R., Kartzinel, T. R., Kurukura, S., Louthan, A. M., Odadi, W. O., Otieno, T. O., Wambua, A. M., … Young, T. P. (2018). Conservation lessons from large-mammal manipulations in East African savannas: the KLEE, UHURU, and GLADE experiments. *Annals of the New York Academy of Sciences*, *1429*(1), 31–49. https://doi.org/10.1111/NYAS.13848

Guo, X., Coops, N. C., Tompalski, P., Nielsen, S. E., Bater, C. W., & John Stadt, J. (2017). Regional mapping of vegetation structure for biodiversity monitoring using airborne lidar data. *Ecological Informatics*, *38*, 50–61. https://doi.org/10.1016/j.ecoinf.2017.01.005

Jackson, H. B., & Fahrig, L. (2015). Are ecologists conducting research at the optimal scale?

Global Ecology and Biogeography, *24*(1), 52–63. https://doi.org/10.1111/GEB.12233

Kunming-Montreal Global biodiversity framework. (2022). *CONFERENCE OF THE PARTIES TO THE CONVENTION ON BIOLOGICAL DIVERSITY*.

LaRue, E. A., Wagner, F. W., Fei, S., Atkins, J. W., Fahey, R. T., Gough, C. M., & Hardiman, B. S. (2020). Compatibility of aerial and terrestrial LiDAR for quantifying forest structural diversity. *Remote Sensing*, *12*(9). https://doi.org/10.3390/RS12091407

Levin, S. A. (1992). The Problem of Pattern and Scale in Ecology: The Robert H. MacArthur Award Lecture. *Ecology*, *73*(6), 1943–1967. https://doi.org/10.2307/1941447

MacArthur, R. H., & MacArthur, J. W. (1961). On Bird Species Diversity. *Ecology*, *42*(3), 594–598. https://doi.org/10.2307/1932254

Marselis, S. M., Tang, H., Armston, J., Abernethy, K., Alonso, A., Barbier, N., Bissiengou, P., Jeffery, K., Kenfack, D., Labri re, N., Lee, S. K., Lewis, S. L., Memiaghe, H., Poulsen, J. R., White, L., & Dubayah, R. (2019). Exploring the relation between remotely sensed vertical canopy structure and tree species diversity in Gabon. *Environmental Research Letters*, *14*(9). https://doi.org/10.1088/1748-9326/ab2dcd

Mittlebach, G. G., Steiner, C. F., Scheiner, S. M., Gross, K. L., Reynolds, H. L., Waide, R. B., Willig, M. R., Dodson, S. I., & Gough, L. (2001). What is the observed relationahip between species richness and productivity? Ecology 82, 2381-2396

McGarigal, K., & Marks, B. J. (1995). *FRAGSTATS: Spatial Pattern Analysis Program for Quantifying Landscape Structure*. https://www.fs.usda.gov/pnw/pubs/pnw_gtr351.pdf

Moudrý, V., Cord, A. F., Gábor, L., Laurin, G. V., Barták, V., Gdulová, K., Malavasi, M., Rocchini, D., Stereńczak, K., Prošek, J., Klápště, P., & Wild, J. (2022). Vegetation structure derived from airborne laser scanning to assess species distribution and habitat suitability:

The way forward. *Diversity and Distributions*. https://doi.org/10.1111/ddi.13644

Oksanen, J. (2022). *Vegan: ecological diversity*.

Pekin, B. K., Jung, J., Villanueva-Rivera, L. J., Pijanowski, B. C., & Ahumada, J. A. (2012). Modeling acoustic diversity using soundscape recordings and LIDAR-derived metrics of vertical forest structure in a neotropical rainforest. *Landscape Ecology*, *27*(10), 1513–1522. https://doi.org/10.1007/S10980-012-9806-4

Rappaport, D. I., Royle, J. A., & Morton, D. C. (2020). Acoustic space occupancy: Combining ecoacoustics and lidar to model biodiversity variation and detection bias across heterogeneous landscapes. *Ecological Indicators*, *113*, 106172. https://doi.org/10.1016/j.ecolind.2020.106172

Sangermano, F. (2022). Acoustic diversity of forested landscapes: Relationships to habitat structure and anthropogenic pressure. *Landscape and Urban Planning*, *226*. https://doi.org/10.1016/J.LANDURBPLAN.2022.104508

Schmitz, O. J., Sylvén, M., Atwood, T. B., Bakker, E. S., Berzaghi, F., Brodie, J. F., Cromsigt, J. P. G. M., Davies, A. B., Leroux, S. J., Schepers, F. J., Smith, F. A., Stark, S., Svenning, J. C., Tilker, A., & Ylänne, H. (2023). Trophic rewilding can expand natural climate solutions. *Nature Climate Change*. https://doi.org/10.1038/s41558-023-01631-6

Simonson, W. D., Allen, H. D., & Coomes, D. A. (2014). Applications of airborne lidar for the assessment of animal species diversity. *Methods in Ecology and Evolution*, *5*(8), 719–729. https://doi.org/10.1111/2041-210X.12219

Steenweg, R., Hebblewhite, M., Kays, R., Ahumada, J., Fisher, J. T., Burton, C., Townsend, S. E., Carbone, C., Rowcliffe, J. M., Whittington, J., Brodie, J., Royle, J. A., Switalski, A., Clevenger, A. P., Heim, N., & Rich, L. N. (2017). Scaling-up camera traps: monitoring the

planet's biodiversity with networks of remote sensors. *Frontiers in Ecology and the Environment*, *15*(1), 26–34. https://doi.org/10.1002/FEE.1448

Veldman, J. W., Overbeck, G. E., Negreiros, D., Mahy, G., Le Stradic, S., Fernandes, G. W., Durigan, G., Buisson, E., Putz, F. E., & Bond, W. J. (2015). Where Tree Planting and Forest Expansion are Bad for Biodiversity and Ecosystem Services. *BioScience*, *65*(10), 1011–1018. https://doi.org/10.1093/biosci/biv118

Wood, S. N. (2017). Generalized additive models: An introduction with R, second edition. In *Generalized Additive Models: An Introduction with R, Second Edition*. Chapman and Hall/CRC. https://doi.org/10.1201/9781315370279

Author Contributions

PBB and ABD conceived the idea and designed the methods; PBB collected and analyzed the data; PBB and ABD wrote the manuscript and gave approval for publication.

Data Accessibility Statement

The input bird survey and lidar point cloud data will be posted to a public data repository. In addition, the version of the python-based data processing pipelines used to produce all the relevant lidar vegetation metrics (*Lidar-Notebooks*: github.com/pbb2291/Lidar-Notebooks) and the R code used for modelling and analysis (github.com/pbb2291/SelenkayDiversity-R) will be archived on Zenodo.

Acknowledgements

We thank Mohanjeet Brar and Gamewatchers Safaris for facilitating access to the study sites and lodging within Selenkay, and we greatly appreciate the efforts and expertise of the ecotourism guides who conducted the bird surveys: Wilson Ole Kasaine, Nicholas Koyeiyo, Daniel Mamai and Lankas Mamai. We also thank Viraj Sikand, CEO of EarthAcre Inc., for facilitating data collection and travel logistics. Funding for the study was gratefully provided through a gift from Emily Kirkland. All UAV flights were performed with permission from KCAA, permit KCAA/OPS/2117/4.

Conflict of Interest Statement

Both authors serve as advisors to a private company, EarthAcre, that aims to monetize ecosystem services within the Selenkay Conservancy. EarthAcre, however, had no input into the analysis or interpretation of the results, nor the writing of the paper. The code and input datasets used in this study will be made publicly available to ensure the transparency of the methods and repeatability of results.

Table 1. Summary statistics (means and standard deviations) of bird diversity data, grouped by soil type and protected status.

Soil	Protected Status	Sample Size (N)	Abundance	Richness	Shannon Index	Evenness
Black	*All Sites*	25	168.68 ± 33.87	41.84 ± 6.21	3.35 ± 0.18	0.9 ± 0.03
	Inside	15	181.4 ± 31.05	43.87 ± 4.96	3.39 ± 0.16	0.9 ± 0.03
	Outside	10	149.6 ± 29.76	38.8 ± 6.89	3.28 ± 0.2	0.9 ± 0.03
Red	*All Sites*	25	160.8 ± 42.93	43.04 ± 6.11	3.43 ± 0.13	0.91 ± 0.02
	Inside	15	172.6 ± 51.13	45.33 ± 6.63	3.44 ± 0.16	0.9 ± 0.02
	Outside	10	143.1 ± 16.39	39.6 ± 3.06	3.42 ± 0.06	0.93 ± 0.01

Table 2. Top 5 correlated variables for Shannon diversity at each scale. ***Bold italics*** mark the strongest Spearman correlation (ρ) achieved for each vegetation structure metric.

		Spearman Correlation with Shannon diversity					
	Metrics	*10 m*	*20 m*	*30 m*	*50 m*	*80 m*	*130 m*
Black Soil	mean_gapsize	0.42	0.61	0.76	0.79	0.81	***0.82***
	sd_gapsize	0.42	0.62	0.71	0.75	0.78	***0.81***
	mean_stdpeakh	0.42	0.59	0.77	0.79	***0.80***	0.79
	meanH_plot	0.23	0.51	0.61	***0.83***	0.79	0.65
	Cover1p5m_plot	0.47	0.70	0.75	***0.83***	0.81	0.76
	gapsize_plot	0.08	0.04	-0.08	0.06	0.28	***0.50***

Red Soil	maxpeakh_plot	0.10	0.03	0.05	0.17	0.26	***0.47***
	ptoh_plot	0.14	0.08	0.15	0.19	0.29	***0.46***
	VDRpeak_plot	0.38	-0.13	-0.12	-0.05	0.18	***0.52***
	stdpeakh_plot	0.09	0.06	0.07	0.13	0.28	***0.45***

Table 3. Top 5 correlated variables for species richness at each scale. ***Bold italics*** mark the strongest Spearman correlation (ρ) achieved for each vegetation structure metric.

		Spearman Correlation with species Richness					
	Metrics	*10 m*	*20 m*	*30 m*	*50 m*	*80 m*	*130 m*
Black Soil	sd_nlayers	0.44	0.58	0.63	***0.69***	0.63	0.58
	cv_nlayers	0.39	0.52	0.59	***0.64***	0.55	0.53
	meanH_plot	0.24	0.36	0.42	0.66	***0.68***	0.52
	stdH_plot	0.22	0.20	0.33	0.57	***0.68***	0.61
	Cover1p5m_plot	0.29	0.44	0.50	0.62	***0.64***	0.53
Red Soil	horzcover_grass	0.43	0.45	0.44	0.52	0.59	***0.60***
	sd_shH_vegtype_grass	-0.49	-0.45	-0.49	-0.61	***-0.67***	-0.67
	sd_cvH_vegtype_grass	-0.47	-0.46	-0.47	-0.50	-0.52	***-0.61***
	50thPerc_plot	-0.33	-0.48	-0.38	-0.41	***-0.60***	-0.56
	75thPerc_plot	-0.43	-0.29	-0.28	-0.37	-0.58	***-0.59***

Table 4. Statistics and descriptions of models of Shannon diversity with UAV-lidar vegetation metrics at increasing spatial scales.

Plot Radius [m]	**R^2**	**Deviance Explained [%]**	**AIC**	**RMSE**	**Significant Variables**
10	0.268	31.5	-49.7	0.133	*sd_CD_AboveG* *sd_herbh*
20	0.325	37.4	-53.4	0.127	*cv_FHD* *cv_CD_AboveG*
30	0.328	37.9	-53.5	0.126	*Cover0p5m_plot*
50	0.558	59.9	-73.6	0.102	*sd_CD_AboveG* *cvpeakh_plot* *cv_FHD*
80	0.493	53.6	-67.2	0.109	*Cover1p5m_plot* *mean_gapsize* *mean_stdpeakh*
130	0.592	63.2	-77.5	0.097	*sd_gapsize* *VDRpeak_plot*

Table 5. Statistics and descriptions of models of log species richness with UAV-lidar vegetation metrics at increasing spatial scales.

Plot Radius [m]	**R^2**	**Deviance Explained [%]**	**AIC**	**RMSE**	**Significant Variables**
10	0.234	30.2	-44.2	0.767	*sd_nlayers* *VDRpeak_plot* *Sd_cvH_vegtype_tree*
20	0.201	24.7	-58.2	0.125	*(X, Y)*
30	0.236	28.2	-60.2	0.122	*sd_nlayers* *(X, Y)*
50	0.362	41.8	-68.0	0.110	*sd_nlayers* *cv_CD_AboveG* *Cvpeakh_plot*
80	0.279	34.5	-61.6	0.117	*meanH_plot* *horzcover_grass*
130	0.388	44.0	-70.2	0.108	*sd_gapsize* *horzcover_grass*

Figures

Figure 1. Overview of the study area and sampling sites around the Selenkay Conservancy, Kenya (a). The 50 bird survey sites and the extent of UAV lidar coverage is shown in (b). Canopy height is overlaid on a lidar terrain model. A Google Earth base map shows the characteristic soil types (black and red) of the region. Polygons of increasing size are shown in (c), colored by buffer radius. The polygons were centered on each bird survey site and used to derive lidar vegetation metrics at a series of increasing scales for comparison with bird diversity data.

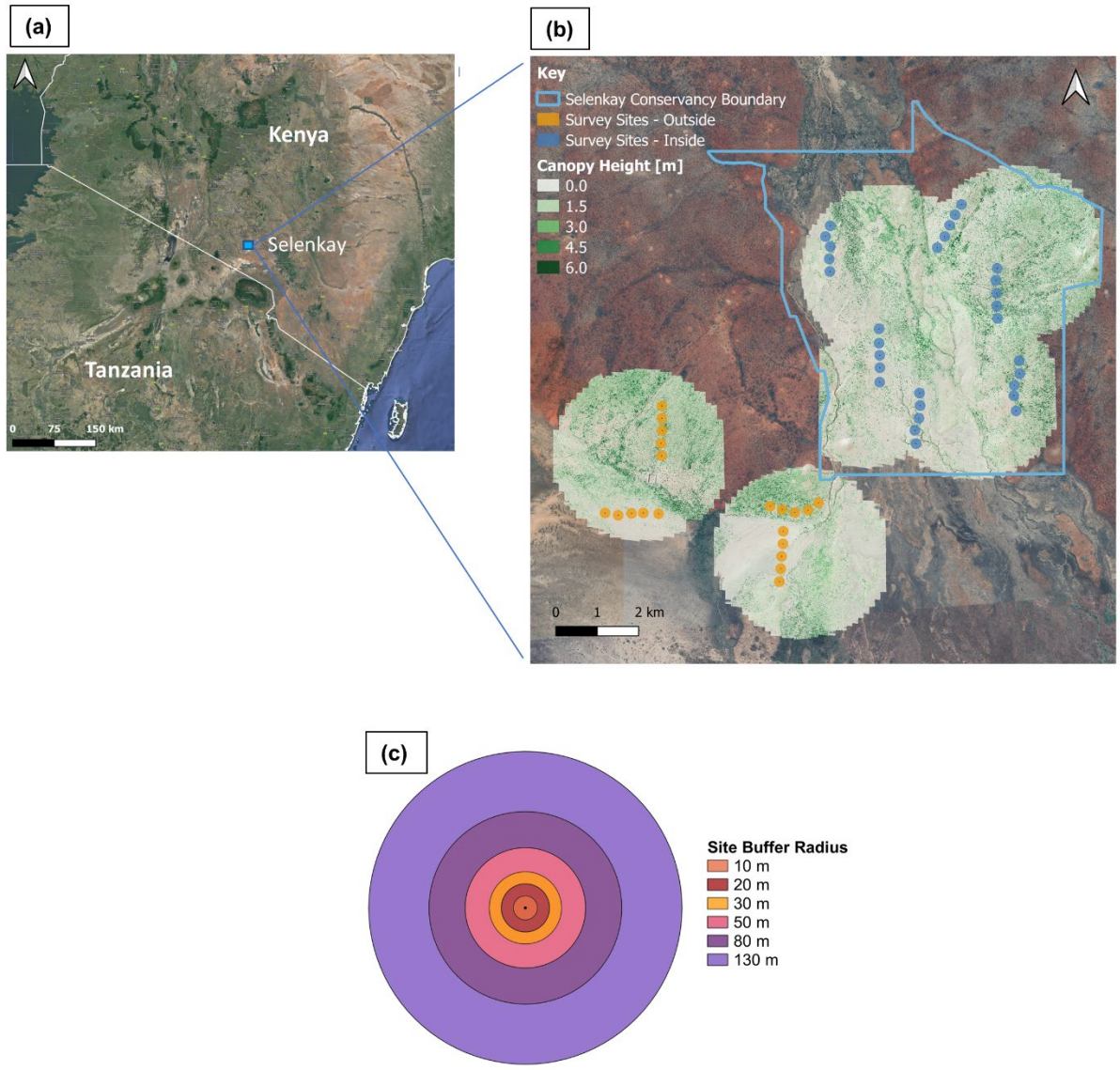

Figure 2. An oblique and top-down view of a 130 m circular plot of UAV-lidar point cloud data (a) over one of the bird survey sites outside of the Selenkay Conservancy, Kenya. Rasterized canopy height and standard deviation in point height per 0.5 m pixel are plotted for the same site (b). A vertical profile of the normalized point density distribution from the point cloud for the entire plot is shown in (c). The peaks and troughs in the point height distribution, smoothed with a gaussian kernel ("gauss1d"), were used to calculate numerous vegetation structure metrics, such as the number of layers (number of peaks), the gap size (maximum distance between peaks), and the herbaceous layer height (upper trough of the lowest identified peak). Point cloud figures were generated with Cloud Compare (*CloudCompare (Version 2.11)*, 2018).

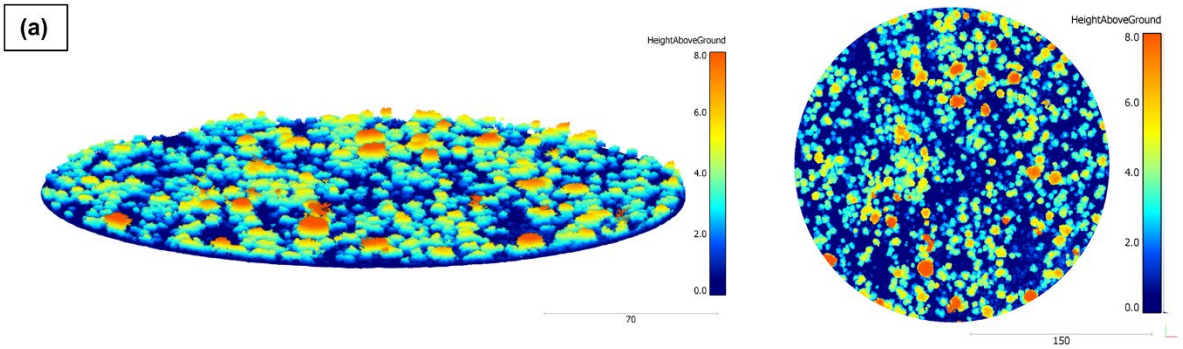
(a)
HeightAboveGround
8.0
6.0
4.0
2.0
0.0
70
HeightAboveGround
8.0
6.0
4.0
2.0
0.0
150

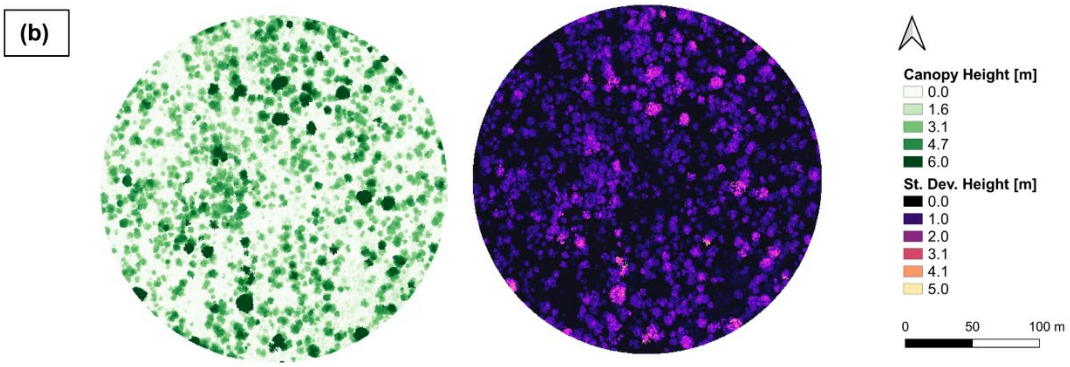
(b)
Canopy Height [m]
0.0
1.6
3.1
4.7
6.0
St. Dev. Height [m]
0.0
1.0
2.0
3.1
4.1
5.0
0
50
100 m

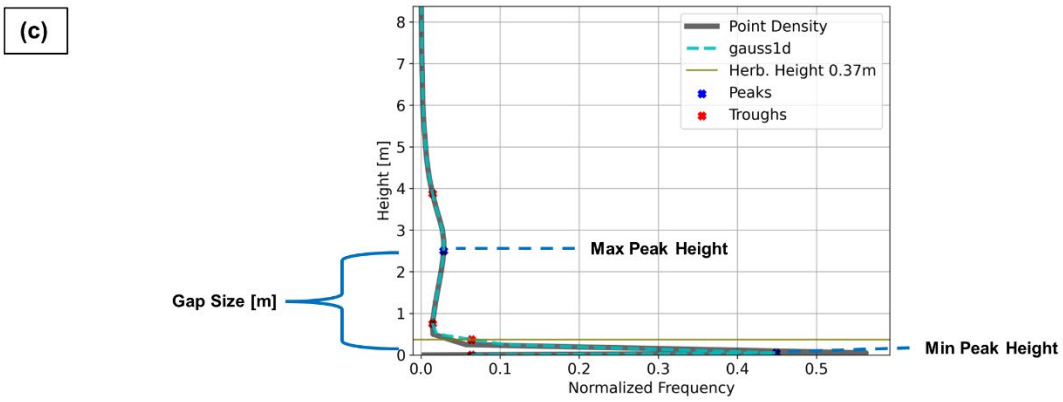
(c)
Point Density
gauss1d
Herb. Height 0.37m
Peaks
Troughs
Height [m]
Max Peak Height
Gap Size [m]
Min Peak Height
Normalized Frequency
0.0
0.1
0.2
0.3
0.4
0.5
0
1
2
3
4
5
6
7
8

Figure 3. Boxplots of bird diversity metrics by soil type (black or red) and protected status (inside or outside the Selenkay Conservancy, Kenya).

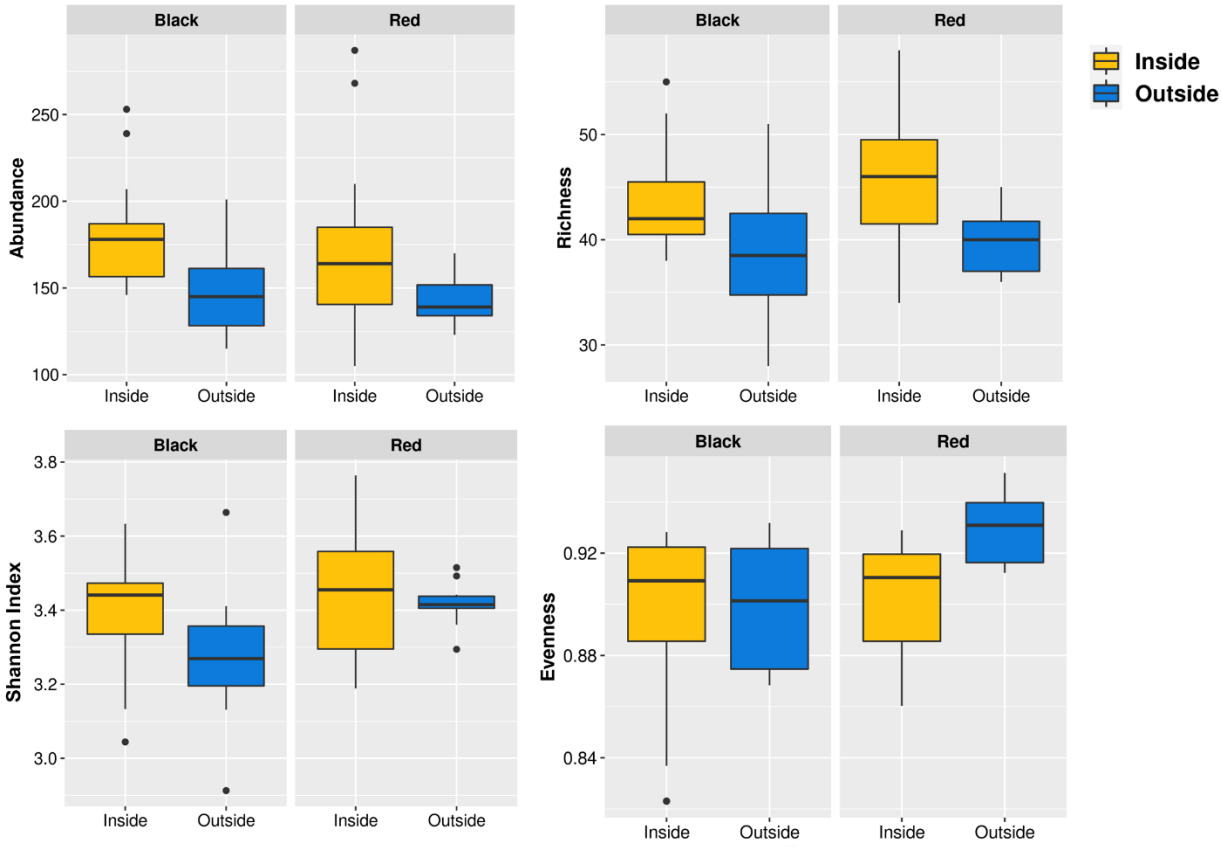

Figure 4. Non-metric multidimensional scaling (NMDS) ordination plots of bird community dissimilarity, grouped by soil type and protected status (inside and outside of the Selenkay Conservancy, Kenya). The ellipses show the 95% confidence interval around each group. An ordination of all 50 sites is shown in panel (a), while panels (b) and (c) show ordination split by soil type (25 sites within each soil).

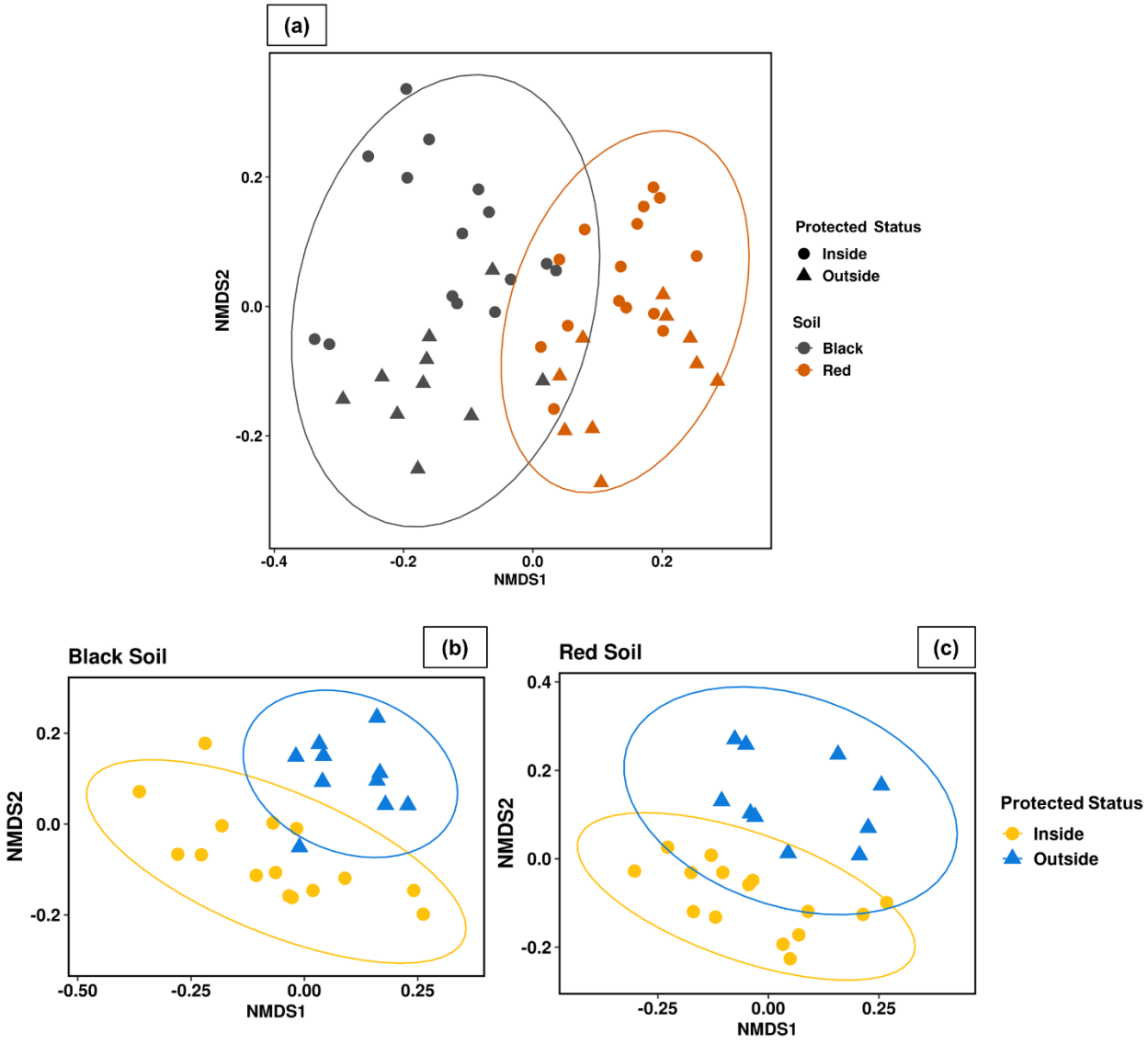

Figure 5. Spearman correlations between the top selected vegetation structure variables and the Shannon diversity index and species richness for birds in and around the Selenkay Conservancy, Kenya, across spatial scales and for each soil type.

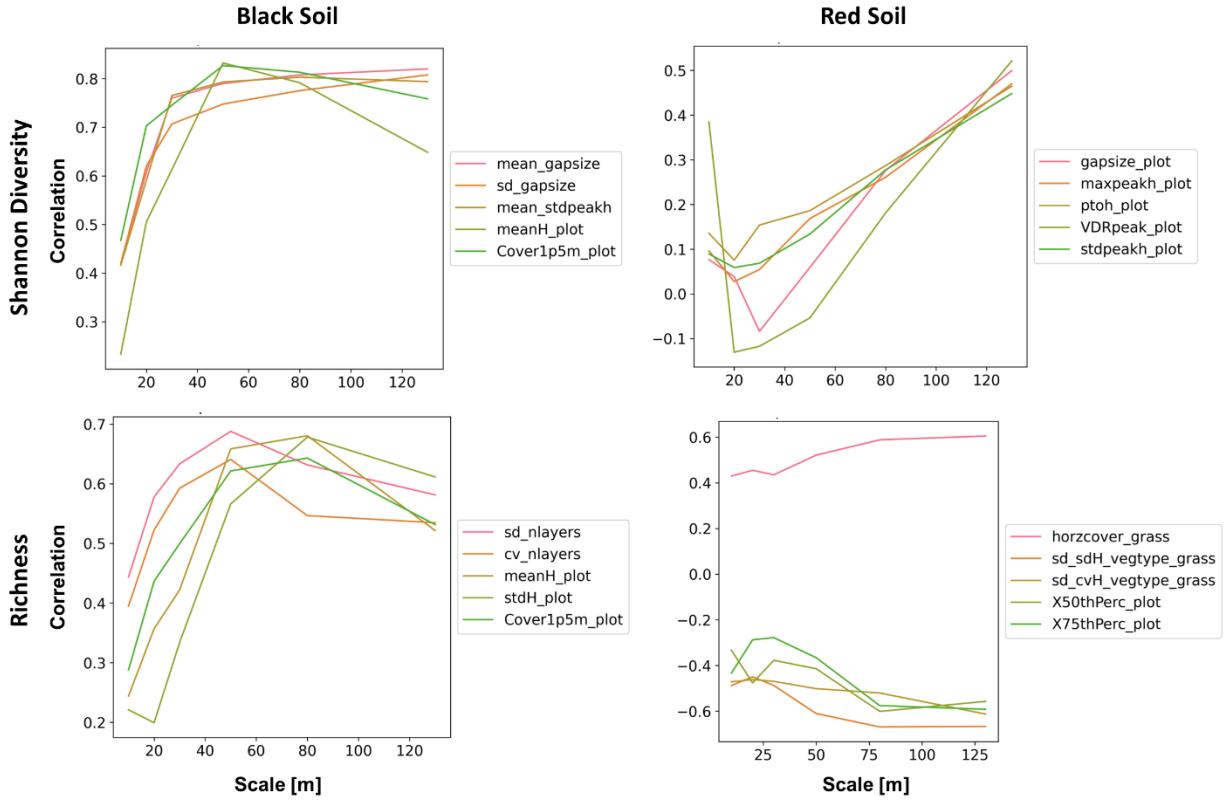

Figure 6. Model fit for a Generalized Additive Model (GAM) of Shannon diversity. This model represents a simplified version of the best model at the 130 m scale from Table 4, following the formula: *shannon ~ sd_gapsize.*(R^2 = 0.53, Explained Deviance = 55.7%, AIC = -72.1, and RMSE = 0.1).

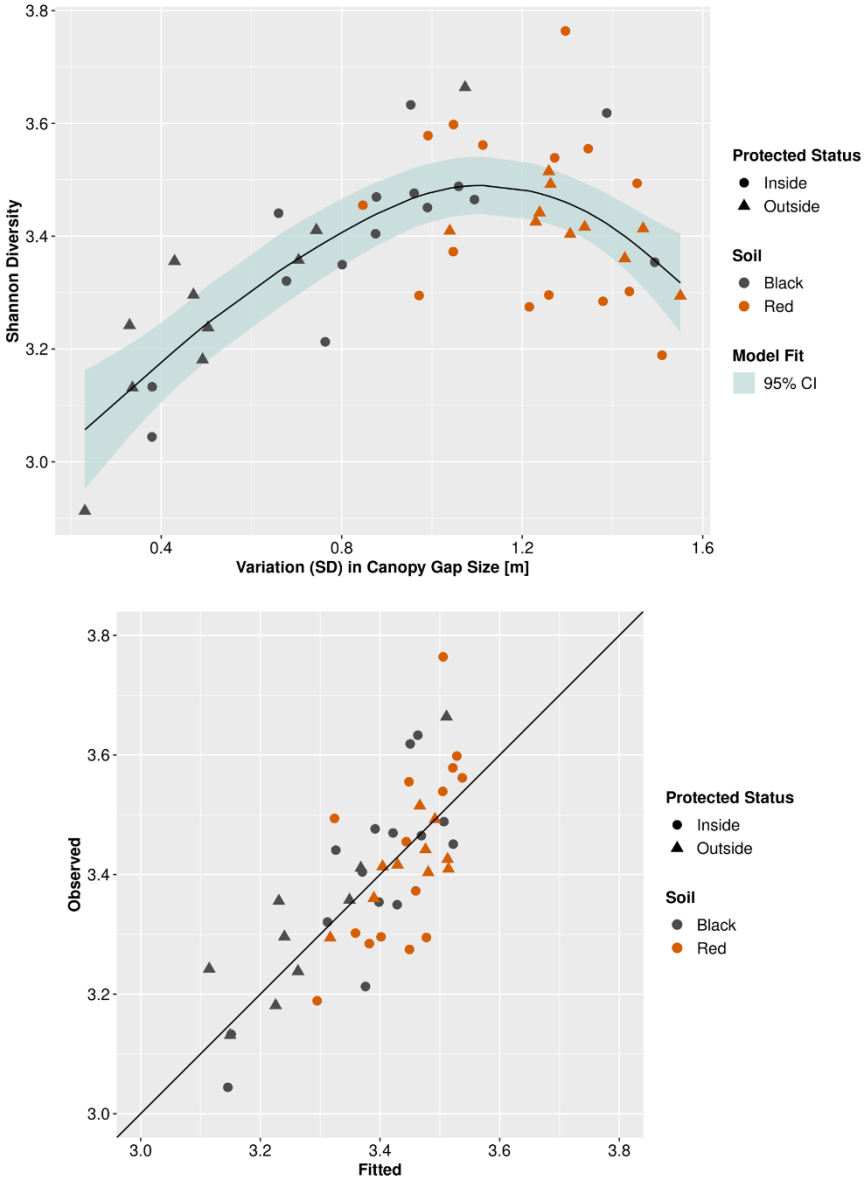

Figure 7. Maps of vertical gap size at 0.5 m resolution and predictions of Shannon diversity of bird communities at 260 m resolution based on the model in Figure 6 (*shannon ~ sd_gapsize*). The area shown is a 3 km by 2 km area from the northwestern portion of the Selenkay Conservancy, Kenya.